VIP Supported Nanoparticles Very Important Paper

DOI: 10.1002/ange.201403585

Monitoring Morphology and Hydrogen Coverage of Nanometric Pt/γ-Al_2O_3 Particles by In Situ HERFD–XANES and Quantum Simulations**

Agnes Gorczyca, Virginie Moizan, Celine Chizallet,* Olivier Proux, William Del Net, Eric Lahera, Jean-Louis Hazemann, Pascal Raybaud, and Yves Joly**

Abstract: *Platinum nanoclusters highly dispersed on γ-alumina are widely used as heterogeneous catalysts. To understand the chemical interplay between the Pt nanoparticles, the support, and the reductive atmosphere, we performed X-ray absorption near edge structure (XANES) in situ experiments recorded in high energy resolution fluorescence detection (HERFD) mode. Spectra are assigned by comparison with simulated XANES spectra on models obtained by molecular dynamics (DFT-MD). We propose platinum cluster morphologies and quantify the hydrogen coverages compatible with XANES spectra recorded at variable hydrogen pressures and temperatures. Using cutting-edge methodologies to assign XANES spectra, this work gives unequalled atomic insights into the characterization of supported nanoclusters.*

Better knowledge of oxide-supported metal nanoclusters is of paramount fundamental and technological importance especially in the field of energy.[1] In particular, highly dispersed platinum nanoparticles supported on γ-alumina are widely used as heterogeneous catalysts, from the laboratory scale to the industrial plant.[1c,2] Their reactivity and selectivity are intimately related to the local geometry and the electronic density of the active sites. As hydrogen is often present in the reactive medium, the metallic nanoparticles are in interaction with both the γ-alumina support and the reductive environment. On such catalysts, the particles are typically sub-nanometric,[3] and the metal sites are even more sensitive to the chemical environment.[4] Herein we show that it is now possible to characterize such systems at the atomic level and in situ. To elucidate their structural and electronic properties, we use X-ray absorption near edge structure (XANES) experiments recorded in high energy resolution fluorescence detection (HERFD)[5] mode. A reasonable quantitative assignment is proposed thanks to ab initio simulations performed on structural models provided by density functional theory molecular dynamics (DFT-MD) approach.

XANES is one of the most appropriate analysis technique to study the local geometry, the oxidation state, and even the electronic structure of nanoclusters, in situ.[6] However, the number of parameters involved and the lack of reference spectra to compare with, makes the need of simulations mandatory to gain quantified insights from experimental data. Typically the unknowns are the atomic positions and the hydrogen coverage, in addition to the fact that the nanoparticles can be adsorbed on different sites and faces of the supporting material. To date, simple models for clusters of well-defined morphology,[3a,4b,7] scarcely accounting for schematic support[6a,d,7,8] and adsorbate[6d,8,9] effects are used in this purpose. More recent studies[10] deal with the effect of adsorbates on supported platinum sub-nanometric particles by XANES spectroscopy. They underline the strong need of more accurate molecular models (including models of the support) to help the interpretation. Herein, we assign in situ HERFD–XANES spectra at the Pt-L_3 edge, recorded at various temperatures and hydrogen pressures, thanks to full multiple scattering (MS) theory calculations using the FDMNES code.[11] The structural models used for such calculations are obtained by DFT-MD using the VASP package,[12] taking into account relevant γ-alumina surfaces and reconstruction effects induced by the hydrogen adsorbate. To our knowledge, this is the first attempt to assign XANES spectra, recorded at this level of resolution, with such accurate models.

The synthesis method to obtain the Pt/γ-Al_2O_3 catalysts is the same than the one employed in Ref. [13]. Chlorine was removed from the support to avoid presence of contaminants. We got a 0.3 wt % Pt loading and a typical cluster size of 1 nm (Supporting Information S3). Hence, we chose Pt_{13} particles as a relevant model for such systems.[4d,14] γ-Al_2O_3 platelets exhibits two main faces (Scheme 1): (100) (ca. 20 % of

[*] A. Gorczyca, Dr. V. Moizan, Dr. C. Chizallet, Dr. P. Raybaud
IFP Energies nouvelles
69360 Solaize (France)
E-mail: virginie.moizan@ifpen.fr
celine.chizallet@ifpen.fr
A. Gorczyca, Dr. J.-L. Hazemann, Dr. Y. Joly
Univ. Grenoble Alpes Inst NEEL
38042 Grenoble (France)
A. Gorczyca, Dr. J.-L. Hazemann, Dr. Y. Joly
CNRS, Inst NEEL
38042 Grenoble (France)
E-mail: yves.joly@neel.cnrs.fr
Dr. O. Proux, W. Del Net, E. Lahera
OSUG, UMS832 CNRS/UJF
38400 Saint Martin d'Hères (France)

[**] This work has been supported by a grant from Labex OSUG@2020 (Investissements d'avenir—ANR10 LABX56). We thank C. Guégan, P. Avenier, and S. Lacombe (IFPEN) for the synthesis of the samples and for fruitful discussions, A. S. Gay (IFPEN) for the STEM-HAADF analysis and I. Kieffer (Institut Néel) for her help during XAS experiments. HERFD-XANES = High energy resolution fluorescence detection–X-ray absorption near edge structure.

Supporting information for this article is available on the WWW under http://dx.doi.org/10.1002/anie.201403585.

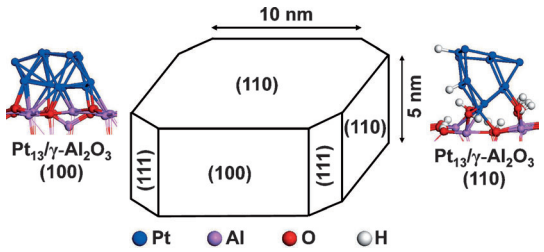

Scheme 1. Schematic representation of alumina platelets,[15b] and two models of Pt_{13} clusters calculated on the main alumina faces (110) and (100) without hydrogen adsorption.[14a,18] Note that on the (110) surface, two hydrogen atoms located on the Pt_{13} cluster were transferred from the hydroxyl groups of the support.

exposed surface) and (110) (ca. 70%). The (111) surface (ca. 10%) is neglected. The hydroxylation state of the (110) surface in reaction conditions considered in this case remains larger than that of the (100) surface.[15] The simulation will assume the location of platinum particles on both surfaces, in the absence of experimental information on that point.

The sample was then analyzed in situ at two temperatures, 25 °C and 500 °C, and two hydrogen pressure values, $P(H_2) = 10^{-5}$ and 1 bar. The higher temperature is typical of operating conditions in catalytic reforming.[1c] We performed the experiment at the Pt-L_3 edge. The benefits of the HERFD collection of the data are well documented.[10a,16] The inset of Figure 1 highlights that a critical feature (detailed below), such as the shoulder at 11574 eV, is revealed only in the HERFD mode. Comparing these spectra with the ones of Pt metal foil, unambiguously highlights the features of the nanometric size of Pt particles (Supporting Information S2).

Decreasing the temperature or increasing $P(H_2)$ makes the main peak at the Pt-L_3 absorption edge, called whiteline, at around 11567 eV broadening, decreasing in maximum intensity and shifting to higher energy. At the same time, the absorption feature at 11574 eV increases. This trend, already reported in the literature,[10a,17] is emphasized in this case

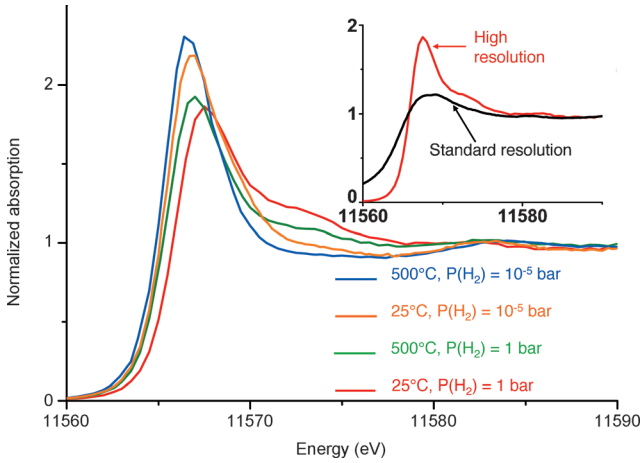

Figure 1. Pt-L_3 edge HERFD–XANES of Pt/Al_2O_3 catalysts recorded at different operating conditions. Inset: spectra recorded at 25 °C and 1 bar of H_2, in HERFD mode (High resolution) and in standard fluorescence mode (Standard resolution).

because we used vacuum to tune $P(H_2)$ while in previous studies, H_2 was diluted in He and the total pressure was kept at atmospheric pressure or above.[8–10] These observations are clearly related to hydrogen adsorption, which follows the expected tendency: the higher $P(H_2)$, or the lower the temperature, the higher the coverage of hydrogen on the particle.

Recent DFT studies suggest that Pt_{13} clusters are almost as stable on both (100) and (110) γ-Al_2O_3 platelets faces in the absence of H_2.[18] Most stable morphologies for supported Pt_{13} clusters are however very different from one face to another: a biplanar structure is preferred on the dehydrated (100) face, whereas a 3D cluster is favorable on the hydrated (110) face (Scheme 1).[14a,18] A hydrogen pressure-dependant reconstruction of the biplanar cluster supported on the γ-Al_2O_3 (100) surface was already suggested by DFT.[4d] For hydrogen contents higher than 20 hydrogen atoms per cluster, the morphology shifts from a biplanar one to a cuboctahedron. To go further, we performed a complementary DFT-MD study on the (110) face and for all possible hydrogen coverage. A thermodynamic diagram was determined using the same method as Mager-Maury et al.[4d] Supporting Information S4 and S5 depict the morphology and stability of these new models as a function of temperature and $P(H_2)$, in comparison with previous findings on the γ-Al_2O_3 (100) face. The stability of the clusters with adsorbed hydrogen is roughly the same on both alumina surfaces. However, the morphologies depend on the nature of γ-Al_2O_3 platelets faces. On the (110) face, the clusters exhibit morphologies with a more pronounced 3D character which may be an effect of the higher hydroxylation state. At high hydrogen coverage (for more than 20 H per cluster), a reconstruction into a cuboctahedron type cluster is also observed though this cluster is more flatten than on (100) surface and closer to the support.

We now turn to the simulation of XANES spectra, using models obtained by DFT as an input for the simulation of XANES spectra. As a preliminary step, to show the sensitivity of the spectroscopy on the models, we compare simulated spectra corresponding to the single alumina (100) face with the experimental spectrum recorded at 25 °C and $P(H_2) =$ 1 bar (Figure 2). The best fit is obtained with a model containing 18 hydrogen atoms adsorbed on the cluster. This fit correctly gives the width of the whiteline, and the existence of structured features at 11574 and 11583 eV. This model still presents a biplanar morphology. A reconstructed cuboctahedron model can be thermodynamically invoked from 20 adsorbed hydrogen atoms (Supporting Information S4.2). The corresponding simulated spectrum (red plot on Figure 2) is not consistent at all with the experimental spectrum, in particular it fails in reproducing 11574 and 11583 eV features. A simulation of the $Pt_{13}H_{18}/\gamma$-Al_2O_3 (100) model, from which all hydrogen atoms were removed (blue in Figure 2) clearly shows the hydrogen coverage impact on the spectra excluding the role of the morphology. Indeed, the simulated whiteline is much too intense, which illustrates that the projected electronic density of state (DOS) on platinum decreases with the presence of hydrogen, as also shown by Bader charge analysis.[4d] Moreover without hydrogen, the spectral features

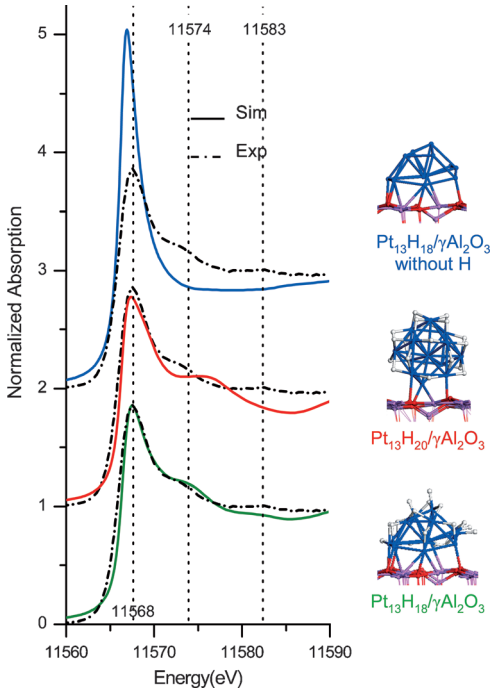

Figure 2. Experimental Pt-L_3 edge HERFD–XANES spectra (dashed line) recorded at 25 °C and $P(H_2) = 1$ bar, and simulated ones (solid line) of the different models displayed on the right side, calculated on γ-Al_2O_3(100). Successive spectra are vertically offset by one unit for clarity.

at 11 574 and 11 583 eV do not appear at all on the simulated spectra.

The full library of models, relative to both alumina faces, is investigated in Supporting Information S6. After a weighted convenient average by the face proportion ratio ((110)/(100) = 7/2), we compare the simulated curves to the experimental spectra recorded at the four given pressure and temperature conditions. Figure 3 shows the best agreements for the four experimental points. By this way we propose a resolution of the hydrogen coverage and the cluster structure, for each experimental condition and on each γ-alumina surface. As expected from the experimental spectra comparison (Figure 1), the hydrogen pressure has a more significant effect on hydrogen coverage than the temperature.

Whatever the conditions, the clusters on the γ-Al_2O_3 (100) face remain biplanar whereas the clusters on the (110) face have a 3D morphology, although strongly distorted compared with the original cluster calculated without hydrogen adsorption (Scheme 1). At lower hydrogen coverage (blue, orange, and green curves in Figure 3), the clusters on the (100) face adsorb slightly more hydrogen atoms than on the (110) face, in agreement with the thermodynamic diagram. This H-coverage difference between Pt_{13} clusters on the two faces comes from the hydroxyl groups of the γ-Al_2O_3 (110) surface. They reduce the negative charge of the metallic clusters[14a] and so the number of electrons available for hydrogen adsorption. The γ-Al_2O_3 (100) surface is not hydroxylated in these conditions, and thus more hydrogen atoms can be adsorbed. In contrast, considering the experiment at 25 °C and $P(H_2) = 1$ bar (Figure 3), with the most significant hydrogen coverage, the cluster on the (110) surface adsorbs more hydrogen atoms than the one on the (100) face. In these (T, $P(H_2)$) conditions, the cluster morphology on the (110) face is changed into a distorted cuboctahedron making available more adsorption sites for hydrogen atoms than for the biplanar morphology.

The biplanar to cuboctahedral cluster reconstruction expected from Mager-Maury et al.[4d] is not reached on the (100) surface according to our experiments but it appears possible on the (110) surface. Note that Mistry et al.[10b] evidenced a reconstruction using a hydrogen pressure much higher (10 bar) than those in our experiments. Clearly, a higher hydrogen coverage is needed to observe a symmetric cuboctahedral morphology, with a characteristic XANES signature, which cannot be reached at the experimental conditions used in our work.

At room temperature, the thermodynamic diagrams overestimate H-coverage (36 H under H_2 and 16 H under vacuum) with respect to the coverage deduced from XANES analysis (18–20 H and 8–10 H respectively, Figure 3) whereas at 500 °C, the diagrams predict lower values (8 H under H_2 and 0 H under vacuum). More specifically around the cluster reconstruction zone, at 500 °C and $P(H_2) = 1$ bar, the hydrogen coverage is lower than at room temperature and under vacuum, which is the opposite in our experimental results. Accuracy limitations of DFT calculations, uncertainties on the temperature/pressure measurements or kinetic effects may explain the shift between thermodynamically predicted data and experimental ones. Thus, it is difficult to have precise information about hydrogen coverage by using calculated thermodynamic diagrams alone, while it is even more difficult

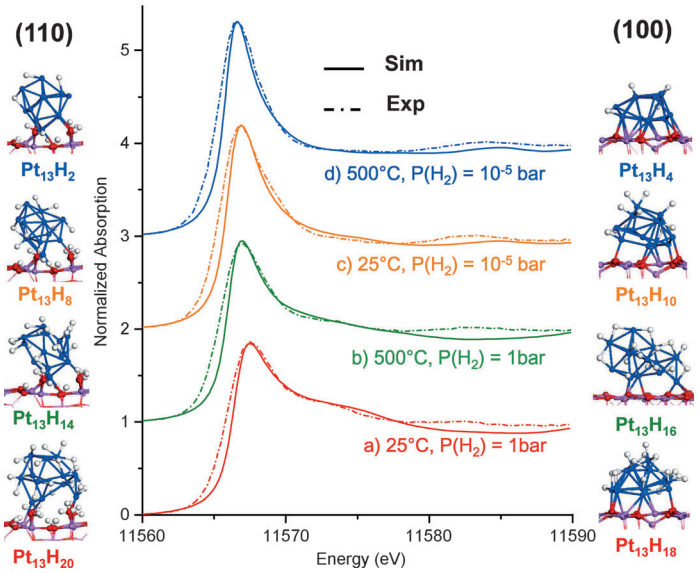

Figure 3. Pt-L_3 edge HERFD–XANES spectra of Pt/Al_2O_3 catalysts recorded in different operating conditions reported in the Figure (dashed line) and best simulated XANES spectra combining models on the (100) face (represented on right) and on the (110) face (represented on left) using the ratio (110)/(100) = 7/2. Successive spectra are vertically offset by one unit for clarity.

by using XAS experiments alone. As a consequence, it is only by combining DFT-MD, XANES simulations and dedicated experiments, that more accurate insights are obtained on the morphologies and the mean hydrogen coverage of the catalyst.

To conclude, in situ HERFD–XANES analysis coupled to DFT-MD calculations allows the discrimination of different morphologies of nanoparticles and to quantify hydrogen coverage, as function of the temperature and hydrogen pressure, taking into account nanometric platinum clusters supported on the two main surfaces of γ-alumina. This work gives unrivalled insights into the influence of hydrogen on morphology, surface structure, and electronic properties of supported metallic nanoclusters, and also brings new methodologies to interpret XANES analysis, used in the characterization of many systems. Hopefully this fine understanding of highly dispersed platinum particles will help for the better control of catalysts under reductive environment.

Experimental Section

The Pt/Al_2O_3 catalyst was prepared by wet impregnation of γ-Al_2O_3 with a solution of H_2PtCl_6. The HERFD–XANES spectra were recorded at the ESRF on the FAME beamline. Ab initio calculations were performed with VASP[12] for the structural part, and with the FDMNES program[11] for the calculation of XANES spectra. Details are given in Supporting Information S7.

Received: March 21, 2014
Published online: July 23, 2014

Keywords: DFT · heterogeneous catalysis · nanoparticles · platinum · XANES

[1] a) G. W. Huber, R. D. Cortright, J. A. Dumesic, *Angew. Chem.* **2004**, *116*, 1575 – 1577; *Angew. Chem. Int. Ed.* **2004**, *43*, 1549 – 1551; b) C. Jensen, D. Buck, H. Dilger, M. Bauer, F. Phillipp, E. Roduner, *Chem. Commun.* **2013**, *49*, 588 – 590; c) J. H. Sinfelt in *Handbook of Heterogeneous Catalysis* (Eds.: G. Ertl, E. Knözinger, J. Weitkamp), Wiley-VCH, Weinheim, **1997**, pp. 1939 – 1955; d) M. Nesselberger, M. Roefzaad, R. Fayçal Hamou, P. U. Biedermann, F. F. Schweinberger, S. Kunz, K. Schloegl, G. K. H. Wiberg, S. Ashton, U. Heiz, K. J. J. Mayrhofer, M. Arenz, *Nat. Mater.* **2013**, *12*, 919 – 924.

[2] G. A. Somorjai, H. Frei, J. Y. Park, *J. Am. Chem. Soc.* **2009**, *131*, 16589 – 16605.

[3] a) B. R. Cuenya, J. R. Croy, S. Mostafa, F. Behafarid, L. Li, Z. Zhang, J. C. Yang, Q. Wang, A. I. Frenkel, *J. Am. Chem. Soc.* **2010**, *132*, 8747 – 8756; b) J. de Graaf, A. J. van Dillen, K. P. de Jong, D. C. Koningsberger, *J. Catal.* **2001**, *203*, 307 – 321; c) S. I. Sanchez, L. D. Menard, A. Bram, J. H. Kang, M. W. Small, R. G. Nuzzo, A. I. Frenkel, *J. Am. Chem. Soc.* **2009**, *131*, 7040 – 7054; d) M. Vaarkamp, J. T. Miller, F. S. Modica, D. C. Koningsberger, *J. Catal.* **1996**, *163*, 294 – 305.

[4] a) S. R. Bare, S. D. Kelly, B. Ravel, N. Greenlay, L. King, G. E. Mickelson, *Phys. Chem. Chem. Phys.* **2010**, *12*, 7702 – 7711; b) F. Behafarid, L. K. Ono, S. Mostafa, J. R. Croy, G. Shafai, S. Hong, T. S. Rahman, S. R. Bare, B. Roldan Cuenya, *Phys. Chem. Chem. Phys.* **2012**, *14*, 11766 – 11779; c) D. C. Koningsberger, M. K. Oudenhuijzen, J. H. Bitter, D. E. Ramaker, *Top. Catal.* **2000**, *10*, 167 – 177; d) C. Mager-Maury, G. Bonnard, C. Chizallet, P. Sautet, P. Raybaud, *ChemCatChem* **2011**, *3*, 200 – 207; e) M. K. Oudenhuijzen, J. A. van Bokhoven, J. T. Miller, D. E. Ramaker, D. C. Koningsberger, *J. Am. Chem. Soc.* **2005**, *127*, 1530 – 1540; f) M. W. Small, S. I. Sanchez, N. S. Marinkovic, A. I. Frenkel, R. G. Nuzzo, *ACS Nano* **2012**, *6*, 5583 – 5595.

[5] a) P. Glatzel, M. Sikora, G. Smolentsev, M. Fernández-García, *Catal. Today* **2009**, *145*, 294 – 299; b) J.-L. Hazemann, O. Proux, V. Nassif, H. Palancher, E. Lahera, C. Da Silva, A. Braillard, D. Testemale, M.-A. Diot, I. Alliot, W. Del Net, A. Manceau, F. Gelebart, M. Morand, Q. Dermigny, A. Shukla, *J. Synchrotron Radiat.* **2009**, *16*, 283 – 292; c) I. Llorens, E. Lahera, W. Delnet, O. Proux, A. Braillard, J. L. Hazemann, A. Prat, D. Testemale, Q. Dermigny, F. Gelebart, M. Morand, A. Shukla, N. Bardou, O. Ulrich, S. Arnaud, J.-F. Berar, N. Boudet, B. Caillot, P. Chaurand, J. Rose, E. Doelsch, P. Martin, P. L. Solari, *Rev. Sci. Instrum.* **2012**, *83*, 063104; d) J. Singh, M. Tromp, O. V. Safonova, P. Glatzel, J. A. van Bokhoven, *Catal. Today* **2009**, *145*, 300 – 306.

[6] a) A. L. Ankudinov, J. J. Rehr, J. J. Low, S. R. Bare, *J. Chem. Phys.* **2002**, *116*, 1911 – 1919; b) S. Bordiga, E. Groppo, G. Agostini, J. A. van Bokhoven, C. Lamberti, *Chem. Rev.* **2013**, *113*, 1736 – 1850; c) A. I. Frenkel, C. W. Hills, R. G. Nuzzo, *J. Phys. Chem. B* **2001**, *105*, 12689 – 12703; d) D. C. Koningsberger, M. K. Oudenhuijzen, J. de Graaf, J. A. van Bokhoven, D. E. Ramaker, *J. Catal.* **2003**, *216*, 178 – 191.

[7] F. Vila, J. J. Rehr, J. Kas, R. G. Nuzzo, A. I. Frenkel, *Phys. Rev. B* **2008**, *78*, 121404.

[8] D. E. Ramaker, J. de Graaf, J. A. R. van Veen, D. C. Koningsberger, *J. Catal.* **2001**, *203*, 7 – 17.

[9] a) A. L. Ankudinov, J. J. Rehr, J. Low, S. R. Bare, *Phys. Rev. Lett.* **2001**, *86*, 1642 – 1645; b) P. Glatzel, J. Singh, K. O. Kvashnina, J. A. van Bokhoven, *J. Am. Chem. Soc.* **2010**, *132*, 2555 – 2557.

[10] a) A. I. Frenkel, M. W. Small, J. G. Smith, R. G. Nuzzo, K. O. Kvashnina, M. Tromp, *J. Phys. Chem. C* **2013**, *117*, 23286 – 23294; b) H. Mistry, F. Behafarid, S. R. Bare, B. Roldan Cuenya, *ChemCatChem* **2014**, *6*, 348 – 352.

[11] O. Bunău, Y. Joly, *J. Phys. Condens. Matter* **2009**, *21*, 345501.

[12] G. Kresse, J. Hafner, *Phys. Rev. B* **1993**, *47*, 558 – 561.

[13] A. Jahel, P. Avenier, S. Lacombe, J. Olivier-Fourcade, J.-C. Jumas, *J. Catal.* **2010**, *272*, 275 – 286.

[14] a) C. H. Hu, C. Chizallet, C. Mager-Maury, M. Corral-Valero, P. Sautet, H. Toulhoat, P. Raybaud, *J. Catal.* **2010**, *274*, 99 – 110; b) S. D. Kelly, M. E. Charochak, N. Blackwell, S. R. Bare, *J. Phys. Conf. Ser.* **2013**, *10*, 430.

[15] a) M. Digne, P. Sautet, P. Raybaud, P. Euzen, H. Toulhoat, *J. Catal.* **2002**, *211*, 1 – 5; b) M. Digne, P. Sautet, P. Raybaud, P. Euzen, H. Toulhoat, *J. Catal.* **2004**, *226*, 54 – 68.

[16] M. Tromp, J. A. van Bokhoven, O. V. Safonova, F. M. F. De Groot, J. Evans, P. Glatzel, *AIP Conf. Proc.* **2007**, *882*, 651 – 653.

[17] J. Singh, R. C. Nelson, B. C. Vicente, S. L. Scott, J. A. van Bokhoven, *Phys. Chem. Chem. Phys.* **2010**, *12*, 5668 – 5677.

[18] C. Mager-Maury, C. Chizallet, P. Sautet, P. Raybaud, *ACS Catal.* **2012**, *2*, 1346 – 1357.

